A LOW-COST GPS AIDED INERTIAL NAVIGATION SYSTEM FOR VEHICLE APPLICATIONS

Isaac Skog and Peter Händel

KTH Signals, Sensors and Systems, Royal Institute of Technology
SE–100 44 Stockholm, Sweden
phone: + (46) 8 790 8742, fax: + (46) 8 790 7260, email: skog@kth.se.
web: www.s3.kth.se

ABSTRACT

In this paper an approach for integration between GPS and inertial navigation systems (INS) is described. The continuous-time navigation and error equations for an earth-centered earth-fixed INS system are presented. Using zero order hold sampling, the set of equations is discretized. An extended Kalman filter for closed loop integration between the GPS and INS is derived. The filter propagates and estimates the error states, which are fed back to the INS for correction of the internal navigation states. The integration algorithm is implemented on a host PC, which receives the GPS and inertial measurements via the serial port from a tailor made hardware platform, which is briefly discussed. Using a battery operated PC the system is fully mobile and suitable for real-time vehicle navigation. Simulation results of the system are presented.

1. INTRODUCTION

Today many vehicles are equipped with global positioning system (GPS) receivers that constantly can provide the driver with information about the vehicles position with an accuracy in the order of 15-100 meters [1]. However, the GPS receiver has two major weaknesses. The slow update rate, only once a second for most receivers and the sensitivity to blocking of the satellite signals. An inertial navigation system (INS) is an alternative tool for positioning and navigation. A classical reference on low-cost INS for mobile robot applications is [2]. In the opposite of the GPS receiver an INS is self contained and can provide position, velocity and attitude estimates at a high rate, typically 100 times per second [3]. However, due to the integrative nature of the INS, low frequency noise and sensor biases are amplified. The unaided INS may therefore have unbounded position and velocity errors [2]. These complementary properties make an integration of the two systems suitable, which is the topic of this paper.

The primary motivation for the reported work is the in-house need for a GPS aided INS test-bed for education and research in the area of vehicle navigation and performance analysis. A goal is to develop a hardware platform and additional software, which together with a standard host-computer will work as a basic GPS aided INS. From the software skeleton the student/researcher can then build an application meeting their demands. Related work do exist, for example in [4] a field evaluation of a low-cost GPS aided INS installed in a car is presented. In [4], the strap-down INS is integrated with two different GPS solutions (pseudo range and carrier phase differential GPS, respectively) using a Kalman filter.

In this paper a loosely coupled position aided method is proposed which allows the designer to keep the costs low by using an off-the-shelf GPS receiver that provides position estimates employing NMEA (National Marine Electronics Association) data transmission protocol and sentence format. In Section 2, the INS equations and the corresponding error models are introduced. Next the navigation dynamics are discretized in Section 3. Section 4 presents an indirect extended Kalman filter (EKF) for the integration between the GPS and INS data. The INS provides the reference trajectory and output. The EKF then estimates the errors, which are fed back to the INS for correction of its internal states, resulting in a closed loop integration, see Figure 1. Implementation aspects, simulations results and conclusions are presented in Section 5.

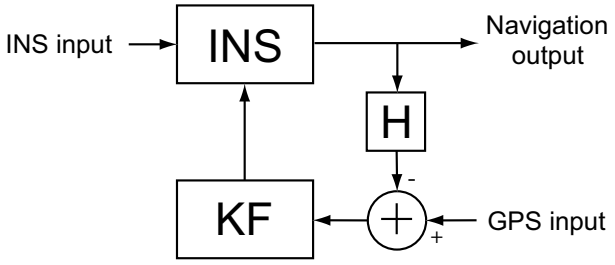

Figure 1: *Loosely coupled position aided closed loop implementation of a GPS aided INS system. KF denotes the extended Kalman filter, and H the map between navigation output and GPS data.*

2. NAVIGATION DYNAMICS

A strap-down INS comprises two distinguished parts. The inertial measurement unit (IMU) housing the accelerometers and gyros. The computational part, consisting of several differential equations, translates the measurements into position, velocity and attitude estimates. The calculations are performed in two steps. From the gyro measurements the directional cosine matrix relating the body coordinate frame to the used navigation frame is propagated. The coordinate rotation matrix is then used when solving the differential equations relating accelerations in the body frame to the navigation coordinate system. An earth-centered earth-fixed (ECEF) navigation coordinate system implementation of the INS has the advantage of producing positions estimate in the same coordinate system as used by the GPS system, which simplifies the integration between the two systems [1].

2.1 Navigation equations

The continuous-time navigation equations in the ECEF frame are [6]

$$\begin{aligned} \dot{\mathbf{r}}^e &= \mathbf{v}^e \\ \dot{\mathbf{v}}^e &= \mathbf{R}_b^e \mathbf{f}^b - 2\,\boldsymbol{\Omega}_{ie}^e \mathbf{v}^e + \mathbf{g}^e \\ \dot{\mathbf{R}}_b^e &= \mathbf{R}_b^e \boldsymbol{\Omega}_{eb}^b \end{aligned} \tag{1}$$

where $\mathbf{r}^e$ and $\mathbf{v}^e$ denote the position and velocity in 3-dimensional ECEF coordinates, respectively. The superscripts *e*, *b* and *i* (that will be used below) are used to denote in which coordinate frame a variable is resolved in, that is the ECEF, body or inertial frame. Further, $\mathbf{f}^b$ is the measured acceleration in the body-frame, $\mathbf{g}^e$ is the position dependent, but known earth acceleration in ECEF coordinates, that may be compensated for. The rotation matrix, $\mathbf{R}_b^e$ transforms a vector in the body frame to the ECEF frame. Although $\mathbf{R}_b^e$ has nine elements, it has only three degrees of freedom and can be uniquely described by the three Euler angles, in the sequel gathered in the vector [5]. The matrices $\boldsymbol{\Omega}_{eb}^b$ and $\boldsymbol{\Omega}_{ie}^e$ are the skew-symmetric matrix representations of the angular rates and , defined such that $\mathbf{a} \times = \boldsymbol{\Omega}_{eb}^b \mathbf{a}$ and $\mathbf{a} \times = \boldsymbol{\Omega}_{ie}^e \mathbf{a}$, where $\mathbf{a}$ is a 3×1 dimensional vector. The matrix $\boldsymbol{\Omega}_{eb}^b$ reads

$$\boldsymbol{\Omega}^b_{eb} = \begin{pmatrix} 0 & -\omega^b_{eb_z} & \omega^b_{eb_y} \\ \omega^b_{eb_z} & 0 & -\omega^b_{eb_x} \\ -\omega^b_{eb_y} & \omega^b_{eb_x} & 0 \end{pmatrix} \tag{2}$$

where the elements $\omega^b_{eb_x}$, $\omega^b_{eb_y}$ and $\omega^b_{eb_z}$ are the angular rates of the body (vehicle) frame relative to the ECEF frame, resolved in the body navigation frame. The matrix, $\boldsymbol{\Omega}^e_{ie}$ has the structure of (2) with the components of ω^b_{eb} replaced by the corresponding components of the earth rotational rate ω^e_{ie}. Since variations in the earth rotational rate ω^e_{ie} are neglectable, $\boldsymbol{\Omega}^e_{ie}$ is assumed constant and known, while $\boldsymbol{\Omega}^b_{eb}$ depends on the body to ECEF angular rates, $\omega^b_{eb} = [\ \omega^b_{eb_x} \quad \omega^b_{eb_y} \quad \omega^b_{eb_z}]^*$ and thus is time-varying. Here $(\cdot)^*$ denotes the transpose operation. The body to ECEF angular rates are obtained by subtracting the angular rate of the earth, resolved in body coordinates from the gyro outputs ω^b_{ib}, that is

$$\omega^e_{eb} = \omega^b_{ib} - \mathbf{R}^b_e \omega^e_{ie} \tag{3}$$

where the rotation matrix from the ECEF to body coordinates is

$$\mathbf{R}^b_e = (\mathbf{R}^e_b)^{-1} = (\mathbf{R}^e_b)^* \tag{4}$$

The last equality is a result of the fact that the directional cosine matrix is an orthonormal matrix (that is, $\mathbf{R}^e_b \mathbf{R}^{e*}_b = \mathbf{I}$).

With reference to Figure 1, the INS inputs are the 3-dimensional measured acceleration in the body frame $\mathbf{f}^b$ and the 3-dimensional angular rates of the body frame with respect to the inertial frame of reference ω^b_{ib}. Further the navigation outputs of Figure 1 are the position, velocity and Euler angles of (1).

2.2 Error equations

Even though the inertial instruments have been calibrated the measured IMU signals will be erroneous, due to environmental variations and instrument degradation. As a result, there are biases in the position and velocity estimates as well as a misalignment between the estimated and true coordinate rotation matrices. The IMU measurement errors can be modelled as a random level, and white Gaussian noise [6], describing the bias and the measurement noise, respectively. Here the IMU sensors are assumed to be the only noise sources in the system. Hence, the noise enters the system equations only through the attitude and velocity state, that is the two last equations in (1). Defining the error state vector $\mathbf{x}(t)$ and the measurement noise vector $\mathbf{u}_c(t)$ as

$$\mathbf{x}(t) = \begin{bmatrix} \mathbf{r}^{e*} & \mathbf{v}^{e*} & * & \mathbf{f}^{b*} & \omega^{b*}_{ib} \end{bmatrix}^* \tag{5}$$

$$\mathbf{u}_c(t) = \begin{bmatrix} \mathbf{u}^*_{acc}(t) & \mathbf{u}^*_{gyro}(t) \end{bmatrix}^* \tag{6}$$

where $\mathbf{r}^e$ denotes the error in position, *et cetera*. The vector is the small angle rotations aligning the actual navigation frame to the computed one. Further, $\mathbf{u}_{acc}(t)$ denotes the accelerometer noise and $\mathbf{u}_{gyro}(t)$ the gyro noise, respectively. Then, if neglecting gravity errors, the navigation error equations can be written as [6]

$$\dot{\mathbf{x}}(t) = \mathbf{F}(t)\ \mathbf{x}(t) + \mathbf{G}(t)\,\mathbf{u}_c(t) \tag{7}$$

where $\mathbf{F}(t)$ is the 15×15 matrix

$$\mathbf{F}(t) = \begin{pmatrix} \mathbf{0}_3 & \mathbf{I}_3 & \mathbf{0}_3 & \mathbf{0}_3 & \mathbf{0}_3 \\ \mathbf{0}_3 & -2\boldsymbol{\Omega}^e_{ie} & -\mathbf{F}^e & \mathbf{R}^e_b & \mathbf{0}_3 \\ \mathbf{0}_3 & \mathbf{0}_3 & -\boldsymbol{\Omega}^e_{ie} & \mathbf{0}_3 & \mathbf{R}^e_b \\ \mathbf{0}_3 & \mathbf{0}_3 & \mathbf{0}_3 & \mathbf{0}_3 & \mathbf{0}_3 \\ \mathbf{0}_3 & \mathbf{0}_3 & \mathbf{0}_3 & \mathbf{0}_3 & \mathbf{0}_3 \end{pmatrix} \tag{8}$$

and $\mathbf{G}(t)$ is of size 15×6

$$\mathbf{G}(t) = \begin{pmatrix} \mathbf{0}_3 & \mathbf{0}_3 \\ \mathbf{R}^e_b & \mathbf{0}_3 \\ \mathbf{0}_3 & \mathbf{R}^e_b \\ \mathbf{0}_3 & \mathbf{0}_3 \\ \mathbf{0}_3 & \mathbf{0}_3 \end{pmatrix} \tag{9}$$

The error equations (7) are time-varying, since $\mathbf{R}^e_b$ depends on the attitude and $\mathbf{F}^e$ (as defined below) on the acceleration of the vehicle. In (8), $\mathbf{I}_3$ ($\mathbf{0}_3$) denotes the unity (zero) matrix of order 3 and $\mathbf{F}^e$ is the skew symmetric matrix, defined as

$$\mathbf{F}^e = \begin{pmatrix} 0 & -f^e_3 & f^e_2 \\ f^e_3 & 0 & -f^e_1 \\ -f^e_2 & f^e_1 & 0 \end{pmatrix} \tag{10}$$

where f^e_ℓ denotes the acceleration along the ℓ:th coordinate axis in the ECEF frame.

The constructed IMU platform houses three separate accelerometers and gyros, therefore the sensor noises are assumed uncorrelated [9]. However, the accelerometers respectively gyros are of the same model and thus assumed to have similar noise characteristics. Let σ^2_{acc} and σ^2_{gyro} denote the variance of the accelerometer and the gyro noise, respectively. Then the covariance matrix, $\mathbf{Q}_c(t)$ of the Gaussian measurement noise $\mathbf{u}_c(t)$ in (6) is given by

$$\mathbf{E}\{\mathbf{u}_c(t+\tau)\,\mathbf{u}^*_c(t)\} = \begin{bmatrix} \sigma^2_{acc}\mathbf{I}_3 & \mathbf{0}_3 \\ \mathbf{0}_3 & \sigma^2_{gyro}\mathbf{I}_3 \end{bmatrix} \delta(\tau) \triangleq \mathbf{Q}_c(\tau) \tag{11}$$

where $\delta(\tau)$ is the Kronecker delta.

3. DISCRETIZATION

The implementation of a GPS aided INS system requires that the navigation and error equations are discretized. First the navigation equations are discretized, where special care is taken to preserve the properties of the rotation matrix. Next the zero-order-hold sampling of the error equation is described.

3.1 Discrete time navigation equations

Zero-order sampling of the position and velocity equations in (1) results in

$$\mathbf{r}^e_{k+1} = \mathbf{r}^e_k + T_s\,\mathbf{v}^e_k \tag{12}$$

$$\mathbf{v}^e_{k+1} = \mathbf{v}^e_k + T_s\,(\mathbf{R}^e_{b,k}\mathbf{f}^b_k - 2\boldsymbol{\Omega}^e_{ie}\mathbf{v}^e_k + \mathbf{g}^e) \tag{13}$$

When discretizing the attitude equation in (1) care must be taken so that the orthogonality constraints of the directional cosine matrix are maintained. Let T_s denote the sampling interval and assume that $\boldsymbol{\Omega}^b_{eb}$ is constant. Then the matrix taking the solution of the attitude differential equation from time instant kT_s to $(k+1)T_s$ is $\exp(\boldsymbol{\Omega}^b_{eb}T_s)$. Hence, the attitude equations can be approximated by

$$\mathbf{R}^e_{b,k+1} = \mathbf{R}^e_{b,k}\exp(\boldsymbol{\Omega}^b_{eb}T_s) \tag{14}$$

By expanding the matrix exponential into an (n,n) Padè approximation the orthogonality constraints of the rotation matrix are preserved [1]. Using a $(2,2)$ Padè approximation the discrete attitude equation becomes

$$\mathbf{R}^e_{b,k+1} = \mathbf{R}^e_{b,k}(2\mathbf{I}_3 + \boldsymbol{\Omega}^b_{eb}T_s)(2\mathbf{I}_3 - \boldsymbol{\Omega}^b_{eb}T_s)^{-1} \tag{15}$$

3.2 Discrete time error equations

Having a continuous-time equation as in (7) with a known solution at time t_0, the solution at a time $t > t_0$ can be represented as [7, 8].

$$\mathbf{x}(t) = \boldsymbol{\Phi}(t,t_0)\ \mathbf{x}(t_0) + \int_{t_0}^{t} \boldsymbol{\Phi}(t,\tau)\,\mathbf{G}(\tau)\,\mathbf{u}_c(\tau)\,d\tau \tag{16}$$

where the state transition matrix $\boldsymbol{\Phi}(t,t_0)$ is defined as the unique solution to $\dot{\boldsymbol{\Phi}}(t,\tau) / \tau = t = \mathbf{F}(t)\,\boldsymbol{\Phi}(t,\tau)$. If the state transition matrix $\mathbf{F}(t)$ in (8) is assumed time invariant, the homogenous differential equation has the solution of the matrix exponential function, that is $\boldsymbol{\Phi}(t,\tau) = \exp(\mathbf{F}\cdot(t-t_0))$ [8]. In the case of $\mathbf{F}(t)$ being time varying, $\mathbf{F}(t)$ can be approximated as a constant matrix $\mathbf{F}$ between the sampling instants, if the sample rate is high compared to the rate

of change in $\mathbf{F}(t)$. Using the power series definition of the matrix exponential, the state transition matrix between time instants kT_s and $(k+1)T_s$ can be approximated as

$$\mathbf{\Phi}((k+1)T_s, kT_s) \approx \mathbf{I}_{15} + \mathbf{F}(kT_s)T_s \tag{17}$$

Hence, the discrete-time error equation becomes

$$\mathbf{x}_{k+1} = \mathbf{\Psi}_k \ \ \mathbf{x}_k + \mathbf{u}_{d,k} \tag{18}$$

where the state transition matrix $\mathbf{\Psi}_k = \mathbf{\Phi}((k+1)T_s, kT_s)$ is approximated as in (17) and the discrete-time process noise, $\mathbf{u}_k$ is

$$\mathbf{u}_{d,k} = \int_{kT_s}^{(k+1)T_s} \mathbf{\Phi}((k+1)T_s, s)\mathbf{G}(s)\mathbf{u}_c(s)ds \tag{19}$$

Since $\mathbf{u}_{d,k}$ is a linear combination of Gaussian noise, it is Gaussian distributed and described by its first and second order moments. The mean of $\mathbf{u}_{d,k}$ is zero, since $\mathbf{u}_c(t)$ is assumed zero mean. Applying the definition of covariance and assuming T_s small, the covariance of the discrete-time noise $\mathbf{Q}_{d,k}$ can be approximated as [1]

$$\begin{aligned} \mathbf{Q}_{d,k} &\approx \mathbf{G}(kT_s)\,\mathbf{Q}_c(kT_s)\,\mathbf{G}^*(kT_s)\,T_s \\ &= \mathrm{diag}(\mathbf{0}_3, \ {}^2_{acc}\mathbf{I}_3, \ {}^2_{gyro}\mathbf{I}_3, \mathbf{0}_6) \end{aligned} \tag{20}$$

where $\mathrm{diag}(\cdot)$ denotes a block diagonal matrix. The last equality is a result of the orthonormality property of the rotation matrix $\mathbf{R}^e_b$, and that $\mathbf{Q}_c(t)$ is a diagonal matrix according to (11).

The definition of the state observation equation is straightforward since the GPS position estimate is used, and not the pseudo ranges. Let $\mathbf{y}$ be the difference between the GPS and INS position estimate and $\mathbf{w}_{d,k}$ the error in the GPS position estimates. Then the observation equation can be written as

$$\mathbf{y}_k = \mathbf{H}_k \ \ \mathbf{x}_k + \mathbf{w}_{d,k} \tag{21}$$

with the state observation matrix $\mathbf{H}_k$ of size 3×15, defined as

$$\mathbf{H}_k = \begin{cases} [\mathbf{I}_3 \ \ \mathbf{0}_{3\times 12}], & k = n\ell, \ n = 1,2,3... \\ \mathbf{0}_{3\times 15}, & \text{otherwise} \end{cases} \tag{22}$$

where ℓ denotes the ratio between the INS and GPS sampling frequency.

4. EXTENDED KALMAN FILTERING

The discrete non-linear navigation equations (12), (13) and (15) can be written as

$$\mathbf{z}_{k+1} = c(\mathbf{z}_k, \mathbf{a}_k) + \mathbf{u}'_k \tag{23}$$

where $c(\cdot,\cdot)$ denotes the dynamics, $\mathbf{z}_k$ is the navigation system outputs: position, velocity and Euler angles defining the rotation matrix $\mathbf{R}^e_b$, that is the 9-element vector

$$\mathbf{z}_k = \begin{bmatrix} \mathbf{r}^{e*}_k & \mathbf{v}^{e*}_k & {}^*_k \end{bmatrix}^* \tag{24}$$

Further, the navigation system input is the 6-element vector $\mathbf{a}_k$ which contains the inputs to navigation system, accelerations and angular rates, that is

$$\mathbf{a}_k = \begin{bmatrix} \mathbf{f}^{b*}_k & {}^{b*}_{ib,k} \end{bmatrix}^* \tag{25}$$

The vector $\mathbf{u}'_k$ is the measurement noise of the navigation inputs. Linearization of the navigation equations (23) are first done around a known nominal trajectory, resulting in a linear model for the perturbations away from the true trajectory. To the linear error equations the standard Kalman filter is applied. Then substituting the nominal trajectory with that of the INS estimated trajectory results in an extended Kalman filter. Consider the true state vector $\mathbf{z}_k$ and the measured input $\tilde{\mathbf{a}}_k$ to the system written as

$$\mathbf{z}_k = \mathbf{z}^{nom}_k + \ \ \mathbf{z}_k \tag{26}$$

$$\tilde{\mathbf{a}}_k = \mathbf{a}^{nom}_k + \ \ \mathbf{a}_k \tag{27}$$

where $\mathbf{z}^{nom}_k$ and $\mathbf{a}^{nom}_k$ are the nominal trajectory and input, respectively. The quantity $\mathbf{z}_k$ is the perturbation away from the true trajectory and $\mathbf{a}_k$ the bias of the measurements. Assuming that $\mathbf{z}_k$ and $\mathbf{a}_k$ are small and applying a first order Taylor series expansion of $c(\mathbf{z},\mathbf{a})$, equation (23) can be approximated as

$$\mathbf{z}^{nom}_{k+1} + \ \ \mathbf{z}_{k+1} \approx c(\mathbf{z}^{nom}_k, \mathbf{a}^{nom}_k) + \mathbf{C}_{1,k} \ \ \mathbf{z}_k + \mathbf{C}_{2,k} \ \ \mathbf{a}_k + \mathbf{u}'_k \tag{28}$$

where

$$\mathbf{C}_{1,k} = \left.\frac{c(\mathbf{z},\mathbf{a})}{\mathbf{z}}\right|_{\mathbf{z}=\mathbf{z}^{nom}_k} \qquad \mathbf{C}_{2,k} = \left.\frac{c(\mathbf{z},\mathbf{a})}{\mathbf{a}}\right|_{\mathbf{a}=\mathbf{a}^{nom}_k} \tag{29}$$

The Jacobians of $c(\mathbf{z},\mathbf{a})$ are updated with nominal trajectory and input for each sample. Choosing $\mathbf{z}^{nom}_k$ and $\mathbf{a}^{nom}_k$ to fulfill the deterministic difference equation

$$\mathbf{z}^{nom}_{k+1} = c(\mathbf{z}^{nom}_k, \mathbf{a}^{nom}_k) \tag{30}$$

and substituting (30) into (28) results in a linear model for the error $\mathbf{z}_k$, that is

$$\mathbf{z}_{k+1} = \mathbf{C}_{1,k} \ \ \mathbf{z}_k + \mathbf{C}_{2,k} \ \ \mathbf{a}_k + \mathbf{u}'_k \tag{31}$$

Note that $\mathbf{x}_k = \begin{bmatrix} \mathbf{z}^*_k & \mathbf{a}^*_k \end{bmatrix}^*$, and thus it becomes clear that $\mathbf{C}_{1,k}$ and $\mathbf{C}_{2,k}$ correspond to the upper part of the navigation error state transition matrix $\mathbf{\Psi}_k$. The lower 6×6 block matrix of $\mathbf{\Psi}_k$ is a description of how the IMU biases $\mathbf{a}_k$ develop with time. Since this is a linear model the standard Kalman filter equations can be applied to estimate $\mathbf{x}_k$ [8]. The Kalman filter equations read

$$\begin{bmatrix} \hat{\mathbf{z}}^-_{k+1} \\ \hat{\mathbf{a}}^-_{k+1} \end{bmatrix} = \mathbf{\Psi_k} \begin{bmatrix} \hat{\mathbf{z}}_k \\ \hat{\mathbf{a}}_k \end{bmatrix} \tag{32}$$

$$\begin{bmatrix} \hat{\mathbf{z}}_k \\ \hat{\mathbf{a}}_k \end{bmatrix} = \begin{bmatrix} \hat{\mathbf{z}}^-_k \\ \hat{\mathbf{a}}^-_k \end{bmatrix} + \mathbf{K}_{f,k} \left(\mathbf{y}_k - \mathbf{H}_k \begin{bmatrix} \mathbf{z}^{nom}_k \\ \mathbf{a}^{nom}_k \end{bmatrix} - \mathbf{H}_k \begin{bmatrix} \hat{\mathbf{z}}^-_k \\ \hat{\mathbf{a}}^-_k \end{bmatrix} \right) \tag{33}$$

$$\mathbf{K}_{f,k} = \mathbf{P}^-_k \mathbf{H}^*_k (\mathbf{H}_k \mathbf{P}^-_k \mathbf{H}^*_k + \mathbf{R}_{d,k})^{-1} \tag{34}$$

$$\mathbf{P}_k = (\mathbf{I} - \mathbf{K}_{f,k}\mathbf{H}_k)\,\mathbf{P}^-_k \tag{35}$$

$$\mathbf{P}^-_{k+1} = \mathbf{\Psi}_k \mathbf{P_k} \mathbf{\Psi}^*_k + \mathbf{Q}_{d,k} \tag{36}$$

Here $\hat{\mathbf{a}}_k$ denotes the estimated biases in the measurements, *et cetera*. Variables with a minus sign, $(\cdot)^-$ are predicted values, and those with superscript *nom* the one obtained from (30). The matrix $\mathbf{R}_{d,k}$ is the covariance matrix of the error $\mathbf{w}_{d,k}$ in the GPS position estimates $\mathbf{y}_k$. Now adding $\mathbf{z}^{nom}_k$ to both sides of equation (32) and substituting $\mathbf{z}^{nom}_k$ with the current estimate in all equations result in an extended Kalman filter, where the time and filter update for the estimates are given below

$$\hat{\mathbf{z}}^-_{k+1} = c(\hat{\mathbf{z}}_k, \hat{\mathbf{a}}_k) \tag{37}$$

$$\hat{\mathbf{a}}^-_{k+1} = [\mathbf{\Psi}_k]_{10:15,\,10:15} \ \ \hat{\mathbf{a}}_k \tag{38}$$

$$\begin{bmatrix} \hat{\mathbf{z}}_k \\ \hat{\mathbf{a}}_k \end{bmatrix} = \begin{bmatrix} \hat{\mathbf{z}}^-_k \\ \hat{\mathbf{a}}^-_k \end{bmatrix} + \mathbf{K}_{f,k} \left(\mathbf{y}_k - \mathbf{H}_k \begin{bmatrix} \hat{\mathbf{z}}^-_k \\ \mathbf{0}_{6\times 1} \end{bmatrix} \right) \tag{39}$$

The solution to (37) is provided by the INS, since this corresponds to the navigation equations. The vector $\hat{\mathbf{a}}_k$ is the estimate of the true IMU-signal obtained by subtracting the estimated bias from the measured IMU signal. The only obstacle is the time update of navigation state errors $\hat{\mathbf{z}}_k$. If the estimated navigation error states are fed back to the INS for correction of the INS internal states, the corresponding error states can be set to zero [5]. Hence, $\hat{\mathbf{z}}^-_k = \mathbf{0}_{9\times 1}$. The final algorithm for the integration is given in Table 1.

No GPS data available. ($k \neq 100, 200, ...$)

$$\hat{\mathbf{a}}_k^- = \tilde{\mathbf{a}}_k + \hat{\mathbf{a}}_k^-$$
$$\hat{\mathbf{z}}_{k+1}^- = c(\hat{\mathbf{z}}_k^-, \hat{\mathbf{a}}_k^-)$$
$$\hat{\mathbf{a}}_{k+1}^- = [\mathbf{\Psi}_k]_{10:15,10:15} \quad \hat{\mathbf{a}}_k^-$$
$$\mathbf{P}_{k+1}^- = \mathbf{\Psi}_k \mathbf{P}_k^- \mathbf{\Psi}_k^* + \mathbf{Q}_{d,k}$$

GPS data available. ($k = 100, 200, ...$)

$$\mathbf{K}_{f,k} = \mathbf{P}_k^- \mathbf{H}_k^* (\mathbf{H}_k \mathbf{P}_k^- \mathbf{H}_k^* + \mathbf{R}_k)^{-1}$$
$$\begin{bmatrix} \hat{\mathbf{z}}_k \\ \hat{\mathbf{a}}_k \end{bmatrix} = \begin{bmatrix} \mathbf{0}_{9\times 1} \\ \hat{\mathbf{a}}_k^- \end{bmatrix} + \mathbf{K}_{f,k} \left(\mathbf{y}_k - \mathbf{H}_k \begin{bmatrix} \hat{\mathbf{z}}_k^- \\ \mathbf{0}_{6\times 1} \end{bmatrix} \right)$$
$$\hat{\mathbf{z}}_k = \hat{\mathbf{z}}_k^- + \hat{\mathbf{z}}_k$$
$$\hat{\mathbf{a}}_k = \tilde{\mathbf{a}}_k + \hat{\mathbf{a}}_k$$
$$\mathbf{P}_k = (\mathbf{I} - \mathbf{K}_{f,k} \mathbf{H}_k) \mathbf{P}_k^-$$
$$\hat{\mathbf{z}}_{k+1}^- = c(\hat{\mathbf{z}}_k, \hat{\mathbf{a}}_k)$$
$$\hat{\mathbf{a}}_{k+1}^- = [\mathbf{\Psi}_k]_{10:15,10:15} \quad \hat{\mathbf{a}}_k$$
$$\mathbf{P}_{k+1}^- = \mathbf{\Psi}_k \mathbf{P}_k \mathbf{\Psi}_k^* + \mathbf{Q}_{d,k}$$

Table 1: *The algorithm for integration between GPS and INS data, with a ratio between the sample rates equal to* 100 *times.*

PSfrag replacements

5. DESIGN AND CONCLUSIONS

Discrete navigation equations for a direct ECEF INS implementation and the corresponding error model have been derived. Further, an indirect extended Kalman filter algorithm for integration between the position estimates from an off-the-shelf GPS receiver and the INS has been presented.

5.1 Hardware Design

A GPS aided INS platform has been developed in-house, consisting of an off-the-shelf GPS receiver and an in-house IMU platform. The IMU platform comprises state-of-the-art MEMS gyros and accelerometers, and a micro-controller to control the data acquisition. The micro-controller controls the GPS-receiver via an RS232 serial interface. The GPS and INS data are synchronized and sent over a second RS232 serial interface to the host PC, see Figure 2. Using a battery operated PC the system is fully mobile and able to perform real-time signal processing [9]. However, at current state procedures for calculating the different calibration parameters are yet to be implemented and therefor no field tests are available. Below follows a short evaluation of the system for simulated IMU data, corresponding to a typical driving scenario.

5.2 Simulation results

The superiority of the GPS aided system over traditional GPS is illustrated in Figure 3. In Figure 3 the dashed trajectory is the position estimates generated by simulated data as input to the GPS aided INS system. The shown specks are the GPS position and the solid line is the true trajectory. A ratio of 100 times was used between the INS and GPS sample ratio and the GPS position estimates had a standard deviation of ten meters. The biases of the accelerometers and gyros were in the order of 1-2 cm/s^2 respectively 5-10 $^\circ/h$. Not surprisingly, the GPS aided system clearly outperforms the GPS-system.

Our current work is focused on studying and implementing different sensor error models and calibration methods, making the testbed available for field tests. More detailed performance evaluations and results from field tests will be reported elsewhere.

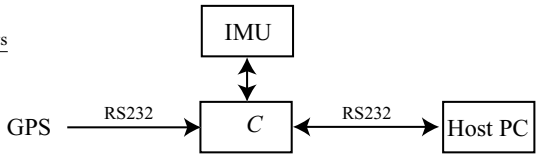

Figure 2: *Block diagram of the hardware.*

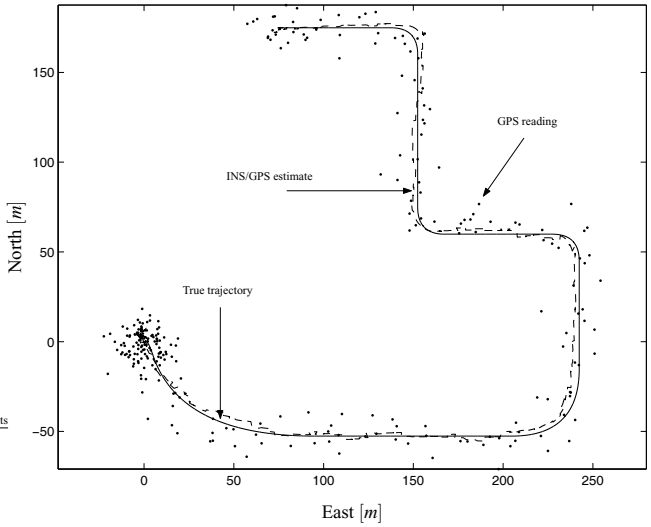

Figure 3: *Estimated and true trajectory of a typical driving sequence. First the car is stationary for* 100 *seconds. Then it makes a wide turn and accelerates to* 18 *km/h, which it keeps until after the last turn. Finally the car slows down and stops. Worth observing is that the accelerometer biases estimates have converged already before the car starts moving, while the gyro biases have not converged until after the last turn.*

REFERENCES

[1] Q. Honghui and J. Moore, "Direct Kalman filtering approach for GPS/INS integration," *IEEE Transactions on Aerospace and Electronic Systems*, vol. 38, pp. 687–693, April. 2002.

[2] B. Barshan and H. Durrant-Whyte, "Inertial navigation systems for mobile robots," in *IEEE Transactions on Robotics and Automation*, June. 1995, vol. 11, pp. 328 – 342.

[3] S. Hong, F. Harashima, S. Kwon, S.B. Choi, M.H. Lee and H. Lee "Estimation of errors in inertial navigation systems with GPS measurements," in *Proc. ISIE 2001, IEEE International Symposium* ,12–16 June. 2001, vol. 3, pp. 1477 – 1483.

[4] R. Dorobantu, B. Zebhauser, "Field evaluation of a low-cost strapdown IMU by means GPS," in *Ortung und Navigation, DGON, Bonn*, 1999, nr. 1, pp. 51 – 65.

[5] J. Farrell and M. Barth, *The Global Positioning System and Inertial Navigation*. McGraw-Hill, 1999.

[6] A. Chatfield, *Fundamentals of High Accuracy Inertial Navigation*. American Institute of Aeronautics and Astronautics, 1997.

[7] K. Åström, B. Wittenmark, *Computer Controlled Systems: Theory and Design*. Prentice-Hall, 1984.

[8] T. Kailath, A.H. Sayed and B. Hassibi, *Linear Estimation*. Prentice-Hall, 2000.

[9] I. Skog, "Development of a low cost GPS aided INS for vehicles," Technical Report, *Dept. of Signals, Sensors and Systems.*, Royal Institut of Technology, Sweden, 2005.